Spatio-temporal hybrid Strauss hardcore point process and application

Morteza Raeisi, Florent Bonneu, Edith Gabriel

Spatio-temporal hybrid Strauss hardcore point process and application

Morteza Raeisi, Florent Bonneu, Edith Gabriel
LMA (Avignon University) & BioSP (INRAE)

April 8, 2021

Abstract

We propose a new point process model that combines, in the spatio-temporal setting, both multi-scaling by hybridization and hardcore distances. Our so-called hybrid Strauss hardcore point process model allows different types of interaction, at different spatial and/or temporal scales, that might be of interest in environmental, biological... applications. The inference and simulation of the model are implemented using the logistic likelihood approach and the birth-death Metropolis-Hastings algorithm. Finally, we apply our model to forest fire occurrences in Spain.

1 Introduction

In point patterns, most types of interaction structure between points can be described by existing models. These models yield point patterns with mainly single-structure, but a few with multi-structure. Interactions with single-structure are often classified into three classes: randomness, clustering and inhibition. Among inhibition processes is the hardcore process. It has some hardcore distance h in which distinct points are not allowed to come closer than a distance h apart. This type of interaction can be modelled by Gibbs point processes as the hardcore or Strauss hardcore point processes and also by Cox point processes as Matérn's hardcore (Matérn, 1960; 1986) or Matérn thinned Cox point processes (Andersen and Hahn, 2016).

In reality, there exist hardcore distances in point patterns that have to be modelled. Spatial point patterns with hardcore property can be found in capillaries studies (Mattfeldt et al., 2006; 2007; 2009), in texture synthesis (Hurtut et al., 2009), in forest fires (Turner, 2009), in cellular networks (Taylor et al., 2012 and Ying et al., 2014), in landslides (Das and Stein, 2016), in modern and contemporary architecture and art (Stoyan, 2016) and in location clustering econometrics (Sweeney and Gomez-Antonio, 2016).

There also exist point patterns with either clustering and inhibition like hardcore interactions at different scales simultaneously (Badreldin et al., 2015; Andersen and Hahn, 2016 and Wang et al., 2020). Wang et al. (2020, sect.

2.4) investigated effect of the hardcore distance on spatial patterns of trees by comparing the pair correlation function curves for different values of hardcore distances in the fitted hybrid Geyer hardcore model. Indeed, the hardcore distance between the points determines the level of clustering in point patterns (Isham, 1984). In other words, hardcore parameter only rules the support of density (Dereudre and Lavancier, 2017).

Raeisi et al. (2019) review spatial and spatio-temporal point processes that model both inhibition and clustering at different scales. Such mutli-structure interactions can be modelled by the spatial hybrid Gibbs point process (Baddeley et al, 2013). In this paper, we aim to extend the spatial Strauss hardcore point process to the spatio-temporal framework and introduce a multi-scale version of it using hybridization approach. As the first work in the scope of the manuscript, Ripley (1988) initiated an application of the Strauss hardcore point process model in a subsequent analysis for the Spanish towns dataset (Glass and Tobler, 1971). We here apply our model to forest fire occurrences.

This paper is organized as follows. In a spatio-temporal framework, we give the background and notations, present examples of Gibbs point processes, introduce the Strauss hardcore point process using cylindrical neighborhood and its multi-scale version (which is the core model of the paper). In Section 3 and 4, we investigate the inference and simulation of our model by extended algorithms to the spatio-temporal context. Finally, we apply our model to a monthly forest fire data in the center of Spain in Section 5.

2 Towards multi-scale Strauss hardcore point processes

Gibbs models are flexible point processes that allow the specification of point interactions via a probability density defined with respect to the unit rate Poisson point process. These models allow to characterize a form of local or Markovian dependence amongst events. Gibbs point processes contain a large class of flexible and natural models that can be applied for:

- Postulating the interaction mechanisms between pairs of points,
- Taking into account clustering, randomness or inhibition structures,
- Combining several structures at different scales with the hybridization approach.

Let $\mathbf{x} = \{(\xi_1, t_1), , ..., (\xi_n, t_n)\}$ be a spatio-temporal point pattern where $(\xi_i, t_i) \in W = S \times T \subset \mathbb{R}^2 \times \mathbb{R}$. We consider $(W, d(\cdot, \cdot))$ where $d((u, v), (u', v')) := \max\{||u - u'||, |v - v'|\}$ for $(u, v), (u', v') \in W$ is a complete, separable metric space. The cylindrical neighbourhood $C_r^q(u, v)$ centred at $(u, v) \in W$ is defined by

$$C_r^q(u, v) = \{(a, b) \in W : ||u - a|| \leq r, |v - b| \leq q\}, \quad (1)$$

where $r, q > 0$ are spatial and temporal radius and $||\cdot||$ denotes the Euclidean distance in $\mathbb{R}^2$ and $|\cdot|$ denotes the usual distance in $\mathbb{R}$. Note that $C_r^q(u,v)$ is a cylinder with centre (u,v), radius r, and height $2q$.

A finite Gibbs point process is a finite simple point process defined with a density $f(\mathbf{x})$ that satisfies the hereditary condition, i.e. $f(\mathbf{x}) > 0 \Rightarrow f(\mathbf{y}) > 0$ for all $\mathbf{y} \subset \mathbf{x}$.

A closely related concept to density functions is Papangelou conditional intensity function (Papangelou, 1974) which is a tool for simulating Gibbs models and infering its parameters. The Papangelou conditional intensity of a spatio-temporal point process on W with density f for $(u,v) \in W$ is defined by

$$\lambda((u,v)|\mathbf{x}) = \frac{f(\mathbf{x} \bigcup (u,v))}{f(\mathbf{x} \backslash (u,v))}, \tag{2}$$

with $a/0 := 0$ for all $a \geq 0$ (Cronie and van Lieshout, 2015).

The Papangelou conditional intensity is also very useful to describe the local interactions in a point pattern, and leads to the notion of a Markov point process which is base of implementation MCMC algorithms for simulation of Gibbs models. We say that the point process has "interactions of range R at (ξ,t)" if points further than R away from (ξ,t) do not contribute to the conditional intensity at (ξ,t). A spatio-temporal Gibbs point process X has a finite interaction range R if the Papangelou conditional intensity satisfies

$$\lambda((u,v)|\mathbf{x}) = \lambda((u,v)|\mathbf{x} \cap C_R^R(u,v)) \tag{3}$$

for all configurations $\mathbf{x}$ of X and all $(u,v) \in W$, where $C_R^R(u,v)$ denotes the cylinder of radius $R > 0$ and height $2R > 0$ centred at (u,v). Spatio-temporal Gibbs models usually have finite interaction range property (spatio-temporal Markov property) and are called in this case Markov point processes (van Lieshout 2002). The finite range property of a spatio-temporal Gibbs model implies that the probability to insert a point (u,v) into $\mathbf{x}$ depends only on some cylindrical neighborhoods of (u,v).

Here, we first review spatio-temporal Gibbs models and then extend the spatial Strauss hardcore model to the spatio-temporal single-(multi-)scales context. We further refer to Dereudre (2019) for more formal introduction of Gibbs point processes.

2.1 Single-scale Gibbs point process models

In the literature, several spatio-temporal Gibbs point process models have been proposed such as the hardcore (Cronie and van Lieshout, 2015), Strauss (Gonzalez et al., 2016), area-interaction (Iftimi et al., 2018), and Geyer (Raeisi et al., 2021) point processes.

A Gibbs point process model explicitly postulates that interactions traduce dependencies between the points of the pattern. The hardcore interaction is one of the simplest type of interactions, which forbids points being too close to each

other. The homogeneous spatio-temporal hardcore point process is defined by the density

$$f(\mathbf{x}) = c\lambda^{n(\mathbf{x})}\mathbb{1}\{||\xi - \xi'|| > h_s \text{ or } |t - t'| > h_t; \forall(\xi, t) \neq (\xi', t') \in \mathbf{x}\}, \quad (4)$$

with respect to a unit rate Poisson point process on $W = S \times T$, where $c > 0$ is a normalizing constant, $\lambda > 0$ is an activity parameter, $h_s, h_t > 0$ are, respectively, the spatial and the temporal hardcore distances and $n(\mathbf{x})$ is the number of points in $\mathbf{x}$. The Papangelou conditional intensity of a homogeneous spatio-temporal hardcore point process for $(u, v) \notin \mathbf{x}$ is obtained

$$\begin{aligned}\lambda((u, v)|\mathbf{x}) &= \lambda\mathbb{1}\{||\xi - u|| > h_s \text{ or } |t - v| > h_t; \forall(\xi, t) \in \mathbf{x}\} \\ &= \lambda \prod_{(\xi,t)\in\mathbf{x}} \mathbb{1}\{||\xi - u|| > h_s \text{ or } |t - v| > h_t\} \\ &= \lambda \prod_{(\xi,t)\in\mathbf{x}} \mathbb{1}\{(\xi, t) \notin C^{h_t}_{h_s}(u, v)\}.\end{aligned} \quad (5)$$

The homogeneous spatio-temporal Strauss point process is defined by density

$$f(\mathbf{x}) = c\lambda^{n(\mathbf{x})}\gamma^{S^q_r(\mathbf{x})}, \quad (6)$$

with respect to a unit rate Poisson point process on $W = S \times T$, where $S^q_r(\mathbf{x}) = \sum_{(\xi,t)\neq(\xi',t')\in\mathbf{x}} \mathbb{1}\{||\xi - \xi'|| \leq r, |t - t'| \leq q\}$ and the Papangelou conditional intensity of the model for $(u, v) \notin \mathbf{x}$ is

$$\lambda((u, v)|\mathbf{x}) = \lambda\gamma^{n[C^q_r(u,v);\mathbf{x}]}, \quad (7)$$

and for $(\xi, t) \in \mathbf{x}$

$$\lambda((\xi, t)|\mathbf{x}) = \lambda\gamma^{n[C^q_r(\xi,t);\mathbf{x}\setminus(\xi,t)]}, \quad (8)$$

where $n[C^q_r(y, z); \mathbf{x}] = \sum_{(\xi,t)\in\mathbf{x}} \mathbb{1}\{||y - \xi|| \leq r, |z - t| \leq q\}$ is the number of points in $\mathbf{x}$ which are in a cylinder $C^q_r(y, z)$. Although the Strauss point process was originally intended as a model of clustering, it can only be used to model inhibition, because the parameter γ cannot be greater than 1. If we take $\gamma > 1$, the density function of Strauss model is not integrable, so it does not define a valid probability density.

Iftimi et al. (2018) defined the homogeneous spatio-temporal area interaction point process by density

$$f(\mathbf{x}) = c\lambda^{n(\mathbf{x})} \prod_{(\xi,t)\in\mathbf{x}} \gamma^{-\ell(\cup_{(\xi,t)\in\mathbf{x}} C^q_r(\xi,t))}, \quad (9)$$

with respect to a unit rate Poisson point process on $W = S \times T$, where ℓ is the Lebesgue measure restricted to $W = S \times T$.

As mentioned, Strauss point process model only achieves the inhibition structure. In spatial framework, two ways are introduced to overcome this problem that we extend to spatio-temporal framework hence defining two new spatio-temporal Gibbs point process models. A first way is to consider an upper bound

for the number of neighboring points that interact. In this case, Raeisi et al. (2021) defined a homogeneous spatio-temporal Geyer saturation point process by density

$$f(\mathbf{x}) = c\lambda^{n(\mathbf{x})} \prod_{(\xi,t)\in\mathbf{x}} \gamma^{min\{s, n^*[C_r^q(\xi,t);\mathbf{x}]\}}, \tag{10}$$

with respect to a unit rate Poisson point process on $W = S\times T$, where s is a saturation parameter and $n^*[C_r^q(\xi,t);\mathbf{x}] = n[C_r^q(\xi,t);\mathbf{x}\backslash(\xi,t)] = \sum_{(u,v)\in\mathbf{x}\backslash(\xi,t)} \mathbb{1}\{||u-\xi||\leq r, |v-t|\leq q\}$.

A second way is to introduce a hardcore condition to the Strauss density (6). Hence, we can define a Strauss hardcore model in spatio-temporal context.

Definition 1. We define the *spatio-temporal Strauss hardcore point process* as the point process with density

$$f(\mathbf{x}) = c\lambda^{n(\mathbf{x})}\gamma^{S_r^q(\mathbf{x})}\mathbb{1}\{||\xi-\xi'||> h_s \text{ or } |t-t'|> h_t; \forall(\xi,t)\neq(\xi',t')\in\mathbf{x}\}, \tag{11}$$

where $0 < h_s < r$ and $0 < h_t < q$.

The model could be used to model clustering patterns with a softer attraction between the points like a pattern with a combination of interaction terms that show repulsion between the points at a small scale and attraction between the points at a larger scale. The Papangelou conditional intensity of a homogeneous spatio-temporal Strauss hardcore point process for $(u,v)\notin\mathbf{x}$ is obtained

$$\begin{aligned}\lambda((u,v)|\mathbf{x}) &= \lambda\gamma^{n[C_r^q(u,v);\mathbf{x}]}\mathbb{1}\{||\xi-u||> h_s \text{ or } |t-v|> h_t; \forall(\xi,t)\in\mathbf{x}\} \\ &= \lambda\gamma^{n[C_r^q(u,v);\mathbf{x}]} \prod_{(\xi,t)\in\mathbf{x}} \mathbb{1}\{(\xi,t)\notin C_{h_s}^{h_t}(u,v)\}.\end{aligned} \tag{12}$$

We can define inhomogeneous versions of all above models by replacing the constant λ by a function $\lambda(\xi,t)$ that expresses a spatio-temporal trend, which can be a function of the coordinates of the points and depends on covariate information.

2.2 Multi-scale Gibbs point process models

Since most natural phenomena exhibit dependence at multiple scales as earthquake (Siino et al., 2017;2018) and forest fire occurrences (Gabriel et al., 2017), single-scale Gibbs point process models are unrealistic in many applications. This motivates statisticians to construct multi-scale generalizations of the classical Gibbs models. Baddeley et al. (2013) proposed hybrid models as a general way to generate multi-scale processes combining Gibbs processes. Given m densities $f_1, f_2, ..., f_m$ of Gibbs point processes, the hybrid density is defined as $f(\mathbf{x}) = cf_1(\mathbf{x})\times f_2(\mathbf{x})\times\cdots\times f_m(\mathbf{x})$ where c is a normalization constant.

Iftimi et al. (2018) extended the hybrid approach for an area-interaction model in spatio-temporal framework where the density is given by

$$f(\mathbf{x}) = c \prod_{(\xi,t)\in\mathbf{x}} \lambda(\xi,t) \prod_{j=1}^{m} \gamma_j^{-\ell(\cup_{(\xi,t)\in\mathbf{x}} C_{r_j}^{q_j}(\xi,t))}, \tag{13}$$

with respect to a unit rate Poisson process on $W = S \times T$, where (r_j, q_j) are pairs of irregular parameters of the model and γ_j are interaction parameters, $j = 1, ..., m$.

In the same way, Raeisi et al. (2021) defined a spatio-temporal multi-scale Geyer saturation point process with density

$$f(\mathbf{x}) = c \prod_{(\xi,t)\in\mathbf{x}} \lambda(\xi, t) \prod_{j=1}^{m} \gamma_j^{min\{s_j, n(C_{r_j}^{q_j}(\xi,t);\mathbf{x})\}} \tag{14}$$

with respect to a unit rate Poisson process on $W = S \times T$, where $c > 0$ is a normalizing constant, $\lambda \geq 0$ is a measurable and bounded function, $\gamma_j > 0$ are the interaction parameters.

As the same way, a hybrid version of spatio-temporal Strauss model can be defined by hybridization.

Definition 2. We define the *spatio-temporal hybrid Strauss point process* with density

$$f(\mathbf{x}) = c \prod_{(\xi,t)\in\mathbf{x}} \lambda(\xi, t) \prod_{j=1}^{m} \gamma_j^{S_{r_j}^{q_j}(\mathbf{x})}, \tag{15}$$

with respect to a unit rate Poisson process on $W = S \times T$.

Note that we called the model (15) hybrid rather than multi-scale. The model (15) can cover inhibition structure because $0 < \gamma_j < 1, \forall j \in \{1, ..., m\}$. However, it can take into account clustering if one of densities in hybrid be a hardcore process (Baddeley et al., 2015, sect. 14.8.6.2).

2.3 Hybrid Strauss hardcore point process

The hybrid Gibbs point process models do not necessarily include m same Gibbs point process models (see Baddeley et al., 2015 sect. 13.8). Badreldin et al. (2015) applied a spatial hybrid model including hardcore process for hardcore structure at very short distances, Geyer process for cluster structure in short to medium distances and a Strauss process for a randomness structure in larger distances to the spatial pattern of the halophytic species distribution in an arid coastal environment. Wang et al. (2020) fitted a spatial hybrid Geyer hardcore point process on the tree spatial distribution patterns. In this section, we extend this type of hybrids to the spatio-temporal context.

Definition 3. We define the *spatio-temporal hybrid Strauss hardcore point process* with density

$$\begin{aligned} f(\mathbf{x}) = c \prod_{(\xi,t)\in\mathbf{x}} \lambda(\xi, t) \prod_{j=1}^{m} \gamma_j^{S_{r_j}^{q_j}(\mathbf{x})} \\ \times \mathbb{1}\{||\xi' - \xi''|| > h_s \text{ or } |t' - t''| > h_t; \forall (\xi', t') \neq (\xi'', t'') \in \mathbf{x}\}, \end{aligned} \tag{16}$$

where $0 < h_s < r_1 < \cdots < r_m$ and $0 < h_t < q_1 < \cdots < q_m$.

In the same way, Papangelou conditional intensity of an inhomogeneous spatio-temporal hybrid Strauss hardcore process for $(u, v) \notin \mathbf{x}$ is obtained

$$\begin{aligned}\lambda((u,v)|\mathbf{x}) &= \lambda(u,v)\prod_{j=1}^{m}\gamma_j^{n[C_{r_j}^{q_j}(u,v);\mathbf{x}]}\mathbb{1}\{||\xi-u||>h_s \text{ or } |t-v|>h_t;\forall(\xi,t)\in\mathbf{x}\}\\ &= \lambda(u,v)\prod_{j=1}^{m}\gamma_j^{n[C_{r_j}^{q_j}(u,v);\mathbf{x}]}\prod_{(\xi,t)\in\mathbf{x}}\mathbb{1}\{(\xi,t)\notin C_{h_s}^{h_t}(u,v)\}.\end{aligned} \tag{17}$$

The conditional intensity of the Gibbs point process models including a hardcore interaction term takes the value zero at some locations. We can thus write that for all parameters of the model

$$\lambda((u,v)|\mathbf{x}) = m((u,v)|\mathbf{x})\lambda^{+}((u,v)|\mathbf{x}), \tag{18}$$

where $m((u,v)|\mathbf{x})$ takes only the values 0 and 1, and $\lambda^{+}((u,v)|\mathbf{x}) > 0$ everywhere.

In the same way as Iftimi et al. (2018) and Raeisi et al. (2021), the spatio-temporal hybrid Strauss hardcore point process (16) is a Markov point process in Ripley-Kelly's (1977) sense at interaction range $\max\{r_m, q_m\}$.

3 Inference

Gibbs point process models involve two types of parameters: regular parameters and irregular parameters. A parameter is called regular if the log likelihood of density is a linear function of that parameter otherwise it is called irregular. Typically, regular parameters determine the 'strength' of the interaction, while irregular parameters determine the 'range' of the interaction. As an example, in the Strauss hardcore point process (11), the trend parameter λ and the interaction γ are regular parameters and the interaction distances r and q and the hardcore distances h_s and h_t are irregular parameters.

To determine the irregular parameters, there are several practical techniques, but no general statistical theory available. Useful technique is maximum profile pseudo-likelihood (Baddeley and Turner, 2000). In the spatio-temporal framework, Iftimi et al. (2018) and Raeisi et al. (2021) selected feasible range of irregular parameters by analyzing the behavior of some summary statistics and the goodness-of-fit of several models with different combinations of parameters. In the spatial framework, the hardcore distance in hybrid Gibbs hardcore point process models can be estimated by the minimum interpoint distance (Baddeley et al., 2013, Lemma 7). Indeed, property (18) states that the hardcore term does not depend on the other parameters in Gibbs point process models. The practical implication is that any parameters governing the hardcore interaction are held fixed (Baddeley et al., 2019, p. 26). However, the lack of uniqueness of the solution in a spatio-temporal framework in most application implies to consider an other methodology. In the spatio-temporal framework, an optimal

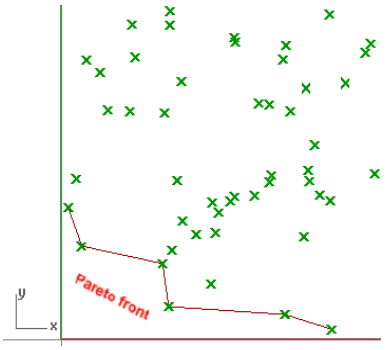

Figure 1: The red line is an example of a Pareto front where the frontier and the area below it are a continuous set of choices. The points on the red line are examples of Pareto-optimal choices of hardcore parameter estimates.

solution (h_s^*, h_t^*) such that it does not exist $h_s > h_s^*$ or $h_t > h_t^*$ where the condition $\{\|\xi - \xi^{'}\| \leq h_s$ and $|t - t^{'}| \leq h_t; \forall(\xi, t) \neq (\xi^{'}, t^{'})\}$ is verified, does not exist in practice. Unlike in the spatial case, the choice of our hardcore parameters needs to analyze the Pareto front of feasible solutions on the graph of spatial and temporal interpoint distances. We compute all pairs of spatial and temporal distances between points and consider these pairs of distances as points in a set S. Let x (resp. y) be the vector of spatial (resp. temporal) distances. To construct the Pareto front, we consider the strict dominance as an ordering operator: we say that x strictly dominates y if $x_i \leq y_i \ \forall i$ and at least one inequality is strict. We then discard any points which are strictly dominated by another element of S to get a reduced set S', so-called the Pareto front. This name is inspired by the way that the remaining points are the "outer shell" of S with the discarded points on the interior (Figure 1). Finally, to estimate the hardcore distance h_s and h_t, we consider the coordinates of a feasible solution on the Pareto front that are as large as possible and with a ratio consistent with our knowledge on interaction mechanisms in practice.

Regular parameters can be estimated using the pseudo-likelihood method (Baddeley and Turner, 2000) or logistic likelihood method (Baddeley et al., 2014) rather than the maximum likelihood method (Ogata and Tanemura, 1981). Due to the advantage of the logistic likelihood over pseudo-likelihood for spatio-temporal Gibbs point processes (Iftimi et al., 2018; Raeisi et al., 2021), we implement the former approach in Raeisi et al. (2021, *Algorithm 2*) for regular parameter estimation of the spatio-temporal hybrid Strauss hardcore point process.

We assume that $\boldsymbol{\theta} = (\log \gamma_1, \log \gamma_2, ..., \log \gamma_m)$ is the logarithm of interaction parameters in spatio-temporal hybrid Strauss hardcore point process (16). The Papangelou conditional intensity of the spatio-temporal hybrid Strauss hardcore

process for $(u,v) \in W = S \times T$ is

$$\lambda((u,v)|\mathbf{x}) = \lambda(u,v) \prod_{j=1}^{m} \gamma_j^{n[C_{r_j}^{q_j}(u,v);\mathbf{x}\setminus(u,v)]} \mathbb{1}\{||\xi-u|| > h_s \text{ or } |t-v| > h_t; \forall(\xi,t) \in \mathbf{x}\setminus(u,v)\}. \tag{19}$$

To estimate $\boldsymbol{\theta}$, due to (18), we just consider the points (u,v) where $m((u,v)|\mathbf{x})$ is equal to 1 in (19). By defining $S_j((u,v),\mathbf{x}) := n[C_{r_j}^{q_j}(u,v); \mathbf{x} \setminus (u,v)]$ in (19), we can thus write $\lambda_{\boldsymbol{\theta}}((u,v)|\mathbf{x}) = \lambda(u,v) \prod_{j=1}^{m} \exp(\theta_j S_j((u,v),\mathbf{x}))$. Hence, the logarithm of the Papangelou conditional intensity of the spatio-temporal hybrid Strauss hardcore point process for $(u,v) \in W$ which satisfies in hardcore condition, i.e. $m((u,v)|\mathbf{x}) = 1$ in (19) , is

$$\begin{aligned} \log \lambda((u,v)|\mathbf{x}) &= \log \lambda(u,v) + \sum_{j=1}^{m} (\log \gamma_j) S_j((u,v),\mathbf{x}) \\ &= \log \lambda(u,v) + \boldsymbol{\theta}^\top \boldsymbol{S}((u,v),\mathbf{x}) \end{aligned} \tag{20}$$

corresponding to a linear model in $\boldsymbol{\theta}$ with offset $\log \lambda(u,v)$ where $\boldsymbol{S}((u,v),\mathbf{x}) = [S_1((u,v),\mathbf{x}), S_2((u,v),\mathbf{x}), ..., S_m((u,v),\mathbf{x})]^\top$ is a sufficient statistics.

Hence, the log logistic likelihood

$$\begin{aligned} \log LL(\mathbf{x},\boldsymbol{d};\boldsymbol{\theta}) = &\sum_{(\xi,t)\in\mathbf{x}} \log \frac{\lambda_{\boldsymbol{\theta}}((\xi,t)|\mathbf{x})}{\lambda_{\boldsymbol{\theta}}((\xi,t)|\mathbf{x}) + \rho(\xi,t)} \\ &+ \sum_{(\xi,t)\in\boldsymbol{d}} \log \frac{\rho(\xi,t)}{\lambda_{\boldsymbol{\theta}}((\xi,t)|\mathbf{x}) + \rho(\xi,t)}, \end{aligned} \tag{21}$$

where $\boldsymbol{d}$ is a realization of a dummy point process independent of point process with known intensity function ρ, is a logistic regression and estimation can be thus implemented by using standard software for GLMs. The logit for the models is

$$\log \frac{\lambda_{\boldsymbol{\theta}}((\xi,t)|\mathbf{x})}{\rho(\xi,t)} = \log \frac{\lambda(\xi,t)}{\rho(\xi,t)} + \sum_{j=1}^{m} \theta_j S_j((\xi,t),\mathbf{x}), \tag{22}$$

which is a linear model in $\boldsymbol{\theta}$ with offset $\log \frac{\lambda(\xi,t)}{\rho(\xi,t)}$. We use *Algorithm 2* in Raeisi et al. (2021) for quadrature points (data and dummy points) such that $m(\cdot|\mathbf{x}) = 1$.

4 Simulation

Due to the markovian property of the spatio-temporal hybrid Strauss hardcore point process (16), its Papangelou conditional intensity at a point thus depends only on that point and its neighbors in $\mathbf{x}$. Hence, We can design simulation approach by MCMC algorithms.

Table 1: Parameter combinations of three hybrid Strauss hardcore point process models used in simulation study.

	Values of parameter			
	Regular parameters		Irregular parameters	
Model	λ	γ	r, q	h_s, h_t
Model 1	70	(0.8,.08)	(0.05,0.1)	(0.01,0.01)
Model 2	50	(1.5,1.5)	(0.05,0.1)	(0.01,0.01)
Model 3	70	(0.5,1.5)	(0.05,0.1)	(0.01,0.01)

4.1 Metropolis-Hastings algorithm

Gibbs point process models can be simulated by Markov chain Monte Carlo algorithms, in particular with a birth-death Metropolis-Hastings algorithm that typically requires only computation of the Papangelou conditional intensity (Møller and Waagepetersen, 2004). Raeisi et al. (2021) extended the birth-death Metropolis-Hastings algorithm to the spatio-temporal context that we adapt here for simulating the spatio-temporal hybrid Strauss hardcore point process.

4.2 Simulation study

We implement the estimation and simulation algorithms in `R` (R Core Team, 2016) and generate simulations of three stationary spatio-temporal hybrid Strauss hardcore point processes specified by a conditional intensity of the form (19) in $W = [0, 1]^3$. The parameter values used for the simulations are reported in Table 1. The spatial and temporal radii r and q, spatial and temporal hardcores h_s and h_t, are treated as known parameters.

We generate 100 simulations of each specified model. Boxplots of parameter estimates λ, γ_1, and γ_2 obtained from the logistic likelihood estimation method for each model are shown in Figure 2. The red horizontal lines represent the true parameter values. Point and interval parameter estimates λ, γ_1, and γ_2 are reported in Table 2. Most of the estimated parameter values are close to the true values for three models. Due to visual and computational comparisons, we conclude that the logistic likelihood approach performs well for spatio-temporal hybrid Strauss hardcore point processes.

5 Application

Forest fire is one of the most complex phenomena from the spatio-temporal modeling point of view. The complexity of forest fire occurrences is due in particular to the existence of multi-scale structures and hardcore distances in space and time.

For instance, changes in vegetation due to forest fires burnt areas affect the probability of fire occurrences during the regeneration period leading to the

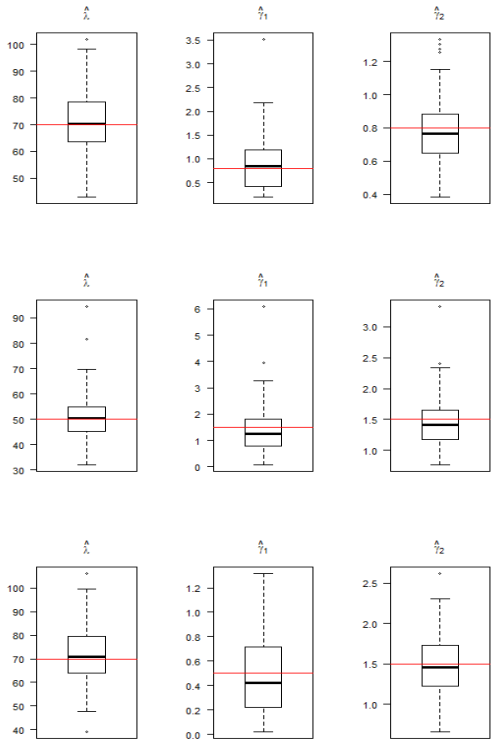

Figure 2: Boxplots of parameter estimates of the hybrid Strauss hardcore point process obtained from the logistic likelihood estimation methods. Up to down: *Model 1*, *Model 2*, and *Model 3*

Table 2: Point and interval parameter estimates of three hybrid Strauss hardcore point process models used in simulation study.

True values	Mean	95% CI
	Model 1	
$\lambda = 70$	71.43	(69.16,73.70)
$\gamma_1 = 0.8$	0.89	(0.78,1.00)
$\gamma_2 = 0.8$	0.78	(0.74,0.82)
	Model 2	
$\lambda = 50$	50.84	(48.99,52.68)
$\gamma_1 = 1.5$	1.41	(1.23,1.60)
$\gamma_2 = 1.5$	1.46	(1.38,1.54)
	Model 3	
$\lambda = 70$	71.67	(69.18,74.15)
$\gamma_1 = 0.5$	0.50	(0.43,0.57)
$\gamma_2 = 1.5$	1.49	(1.42,1.55)

Figure 3: Map of region of Castilla-La Mancha (Spain)

existence of hardcore distances in space-time. It can be also observed the multi-scale structure of clustering and inhibition in the spatio-temporal pattern of the forest fires which discussed in Gabriel et al. (2017).

The main focus of our forest fire pattern analysis is to quantify the interactions across a range of spatio-temporal scales which can be done by using the spatio-temporal hybrid Strauss hardcore process. We apply our model on a forest fire pattern of Castilla-La Mancha in Spain (see Figure 3).

5.1 Study region and dataset

Castilla La Mancha is located in the middle of the Iberian peninsula and the third largest of Spain's autonomous regions representing 15.7% of the Spanish national territory.

5.1.1 Data description

The `clmfires` dataset available in `spatstat` package records the occurrence of forest fires in the region of Castilla-La Mancha (Spain) from 1998 to 2007. This region is approximately 400 by 400 km. The study area was partitioned in pixels of 4×4 km, resulting in a total of 10000 pixels. The `clmfires` dataset have already been used in some academic works devoted to the point process theory (see for example Juan et al., 2010; Gomez-Rubio, 2020, sect. 7.4.2; Myllymäki et al., 2020)

Because of the low precision of fire locations for the years 1998 to 2003 (Gomez-Rubio 2020, sect. 7.4.2), we focus on fires in the period 2004 to 2007. In this period, we consider fires with a burnt area larger than 5 ha. Figure 4 (left) shows the projection of 432 wildfire locations onto the spatial region.

Due to memory constraints and availability of climate covariates in months, we consider monthly fire occurrences. The temporal component of the process

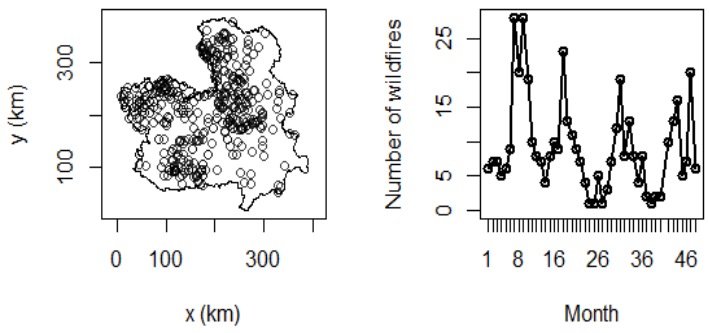

Figure 4: Location (left) and number per month (right) of forest fires recorded during January 2004 to December 2007 with burnt area, space distance and time distance bigger than 5 ha, 0.2 km and 100 $days$, respectively, in Castilla-La Mancha (Spain).

takes integer values from 1 to 48. We thus consider $W = S \times T$ where S is the region of Castilla-la-Mancha and $T = \{1, 2, ..., 48\}$ corresponds to the months since January the first of 2004. Figure 4 (right) shows the temporal fire occurrences over the 48 months. We observe a seasonal period in spring and summer with a large numbers of fires in summer that could be caused to the high temperature and the low precipitation in these seasons and also human-caused fires in summer break.

5.1.2 Environmental covariates

In point pattern analysis, the spatial (spatio-temporal) inhomogeneity of patterns is driven by covariates. The `clmfires` dataset contains four environmental covariates. We consider them in our analysis that include *elevation*, *orientation*, *slope* and *land use*. The *land use* is a factor-valued covariate. Figure 5 is the image plot of these covariates that are fixed during our temporal period.

5.1.3 Climate covariates

We consider weather data freely provided by *WorldClim* database[1] containing monthly maximum temperature ($°C$) and total precipitation (mm) for all the world in *.tif* format. We extract the values of climate covariate for our spatio-temporal study region by `raster` package in `R`. Figure 6 is the image plot of climate covariates on January 2007.

[1] `https://www.worldclim.org`

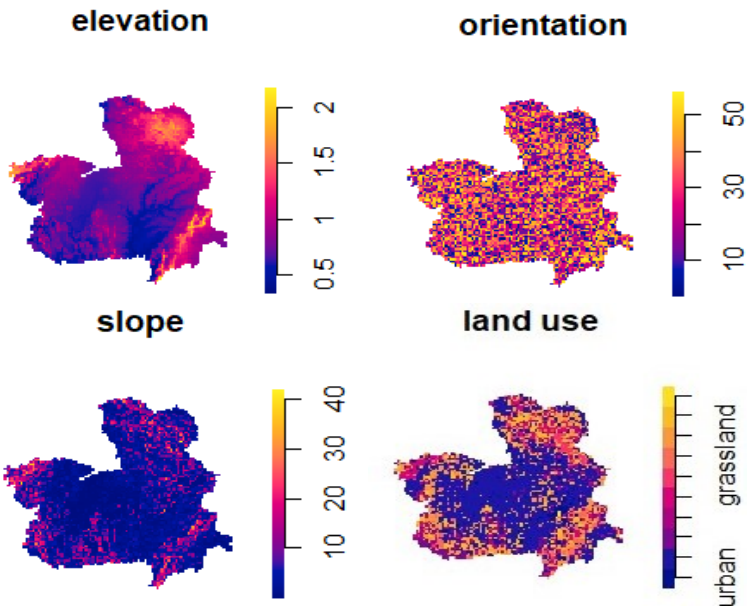

Figure 5: The image plot of covariates *elevation*, *orientation*, slope and *land use*.

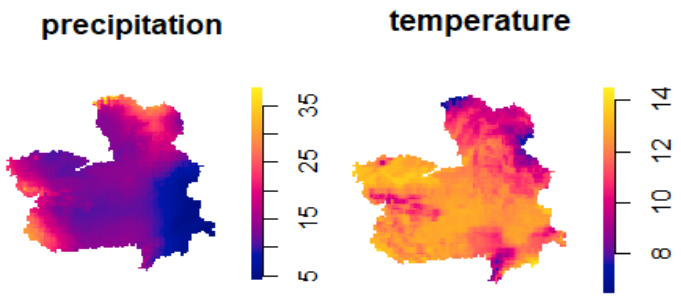

Figure 6: The image plot of covariates *precipitation* and *temperature* on January 2007.

Table 3: Estimated coefficients, standard errors and p-values based on two-tailed Student's t-tests of significant differences from zero.

Coefficients	Estimate	Standard error	p-value
β_0 (intercept)	-8.468	0.298	$< 2 \times 10^{-16}$ ***
β_1 (elevation)	0.546	0.164	0.001 ***
β_2 (orientation)	0.005	0.003	0.114
β_3 (slope)	-0.019	0.01	0.054
β_4 (land use)	-0.009	0.024	0.689
β_5 (precipitation)	-0.007	0.002	0.003 **
β_6 (temperature)	0.054	0.006	$< 2 \times 10^{-16}$ ***

5.2 Estimation

To estimate the parameters of the model, first, we consider that the trend function is a GLM of covariates and use `glm` function in `R`. Then, by an exploratory analysis using spatio-temporal summary statistics we approximate the hardcore parameters and interaction ranges. Finally, we use the logistic likelihood approach described in Section 3 for the regular parameters estimation of the model using the estimated trend function.

5.2.1 Trend estimate

As the same way as Raeisi et al. (2021), the trend term of our model could be written in a loglinear function (the simplest and most popular form) of covariates. Hence, we assume

$$\log \lambda(\xi, t) = \beta_0 + \sum_{k=1}^{6} \beta_k Z_k(\xi, t), \tag{23}$$

where $Z_k(\xi, t)$ are the covariates at point (ξ, t) and β_0, β_k are the coefficients to estimate, with $k = 1, \ldots, 6$. We consider the same values for environmental covariates in months to express them in spatio-temporal context. Since the covariates are available in center of 10000 grids in region study, we restrict our attention on grid centers $\xi_i, i = 1, \ldots, 10000$ and months $t_j = \{1, \ldots, 48\}$ for $j = 1, \ldots, 48$. We consider a Poisson response for our model $N_{ij}|\lambda(\xi_i, t_j) \sim Poisson(\lambda(\xi_i, t_j))$, where $\xi_i, i = 1, \ldots, 10000$ are the grid centers, $t_j \in \{1, \ldots, 48\}$ are the months and N_{ij} is the number of forest fires in i^{th} grid at month t_j.

The systematic component of the GLM specifies a relationship between the mean response and the covariates. In particular, the systematic component consists of a link function (e.g. log function) that transforms the mean response and then expresses this transformed mean in terms of a linear function of the covariates. In our notation, this is given by (23). A straightforward way to fit a GLM in `R` is to use the function `glm`. Table 3 reports the estimated coefficients for the fitted GLM (23) on covariates.

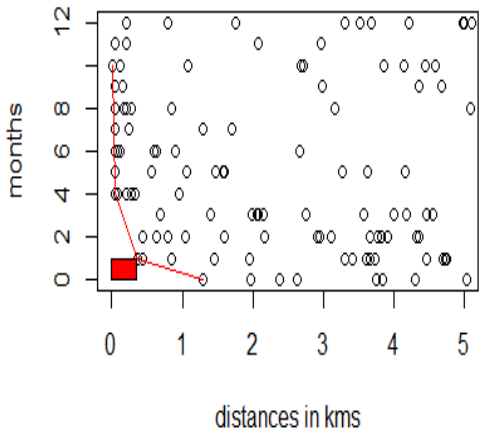

Figure 7: The red line is Pareto front corresponds to all pair spatial and temporal distances of our data set.

5.2.2 Irregular parameter estimates

There is no common method for estimating irregular parameters in spatial or spatio-temporal Gibbs point process models. Here we considered several combinations of ad-hoc values within a reasonable range and select the optimal irregular parameters according to the Akaike's Information Criterion (AIC) of the fitted model (Raeisi et al., 2021).

By using Pareto front approach discussed in Section 3, we consider $h_s = 0.35$ km and $h_t = 1$ $month$. See Figure 7. We chose configurations of feasible values for the nuisance parameters m, r_j and q_j, $j = 1, \ldots, m$ using a preliminary spatio-temporal exploratory analysis of the interaction ranges done with the inhomogeneous pair correlation function, the maximum nearest neighbor distance and the temporal auto-correlation function.

5.2.3 Regular parameter estimates

We consider the logistic likelihood method investigared in Section 3 to estimate the regular parameters. We simulate dummy points from an inhomogeneous Poisson point process with intensity $\rho(\xi, t) = C\lambda(\xi, t)/\nu$ where $C = 4$ by a classical rule of thumb in the logistic likelihood approach and $\nu = 4 \times 4 \times 1$ (area of a grid cell multiplied by 1 month).

We fitted the spatio-temporal hybrid Strauss point process model for a range

Table 4: Parameter estimates for $m = 6$.

	Irregular parameters					
r	0.5	1	1.5	6	15	20
q	2	4	6	8	12	15
	Estimated regular parameters					
	$\hat{\gamma}_1 = 2.56$	$\hat{\gamma}_2 = 2.24$	$\hat{\gamma}_3 = 4.65$	$\hat{\gamma}_4 = 0.88$	$\hat{\gamma}_5 = 1.17$	$\hat{\gamma}_5 = 0.81$

of ad-hoc values $r_j \in [0, 20]$, q_j in $\{2, ..., 15\}$ because possible correlation for time lags is as big as 15 months. The minimum AIC is obtained for the combination given in Table 4.

5.3 Goodness-of-fit

The goodness-of-fit for a model is accomplished by simulating new point patterns from the fitted model. The first diagnostic can be formulate by the summary statistics of point processes. For each simulated realization of points, we compute a spatio-temporal second-order summary statistic such as the (inhomogeneous) pair correlation function (g-function) or K-function. We then compare the distribution of summary statistics for the simulated points and original points.

Occasionally, apart from the second-order distribution characteristic described by the g- and K-functions, higher-order interactions are also likely to exist in a spatio-temporal point patterns (Gonzalez et al., 2016). In this case, other high-order summary statistics such as spatio-temporal nearest-neighbor distance distribution function and empty-space function (Cronie and van Lieshout, 2015) can also be fitted simultaneously to achieve a better approximation. According to the general empirical experience in spatial point process statistics (Stoyan, 1992), the second-order distribution characteristic carries most of the information on a spatial structure. Thus, only the g-function is considered here for simplicity.

To do this, we generate n_{sim} simulations from a fitted hybrid Strauss hard-core model. We then compute the corresponding second-order summary statistics for each simulated point pattern denoted by $g_i(u, v), i \in \{1, ..., n_{sim}\}$. For each value of the spatio-temporal distance (u, v), upper and lower critical envelopes of the observed summary statistics are computed pointwise by sorting the values of

$$U(u, v) = \max_{1 \leq i \leq n_{sim}} g_i(u, v), \quad L(u, v) = \min_{1 \leq i \leq n_{sim}} g_i(u, v). \tag{24}$$

If the observed curve of $g_{obs}(u, v)$ lies outside the envelope, it means that the fitted model does not describe properly the characteristics of the data. Indeed, simulated envelopes generate significance bands of the second-order summary statistics rather than confidence intervals.

We generated $n_{sim} = 99$ simulations from our fitted model. Figure 8 shows the spatio-temporal inhomogeneous g-function computed on our dataset (green)

and the envelopes obtained from our hybrid Strauss hardcore model (light grey); $g_{obs}(u, v)$ lies inside the envelopes, meaning that the fitted model seems to describe properly the spatio-temporal structure of the data.

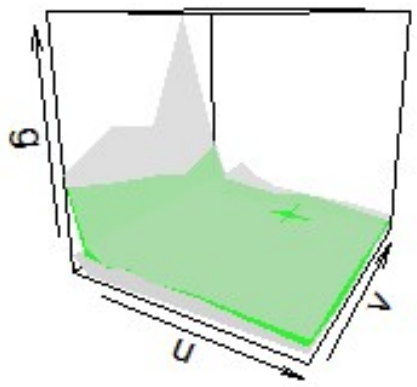

Figure 8: Envelopes of the spatio-temporal inhomogeneous pair correlation function for the simulated spatio-temporal hybrid Strauss hardcore point process according to the estimated parameters. Temporal separations are in month and spatial distances are in kilometer.

In addition, we compute global envelopes and p-value of the spatio-temporal g-functions based on the Extreme Rank Length (ERL) measure defined in Myllymäki et al. (2017) and implemented in the `R` package GET (Myllymäki and Mrkvička, 2020). For each point pattern, we consider the long vector T_i, $i = 1, \ldots, n_{sim}$ (resp. T_{obs}) merging the $g_i(\cdot, v)$ (resp. $g_{obs}(\cdot, v)$) estimates for all considered values h_t. The ERL measure of vector T_i (resp. T_{obs}) of length n_{st} is defined as

$$E_i = \frac{1}{n_{ns}} \sum_{j=1}^{n_{st}} \mathbb{1}\{R_j \prec R_i\},$$

where R_i is the vector of pointwise ordered ranks and $\prec$ is an ordering operator (Myllymäki et al., 2017; Myllymäki and Mrkvička, 2020). The final p-value is obtained by

$$p_{erl} = \frac{1 + \sum_{i=1}^{n_{sim}} \mathbb{1}\{E_i \geq E_{obs}\}}{n_{sim} + 1}.$$

Due to the global p-value $p_{erl} = 0.11$ and the absence of significant regions, that corresponds here to pairs of spatial and temporal distances where the statistics is significantly above or below the envelopes (see Figure 9 and GET package), we conclude that our hybrid Strauss hardcore model can not be rejected.

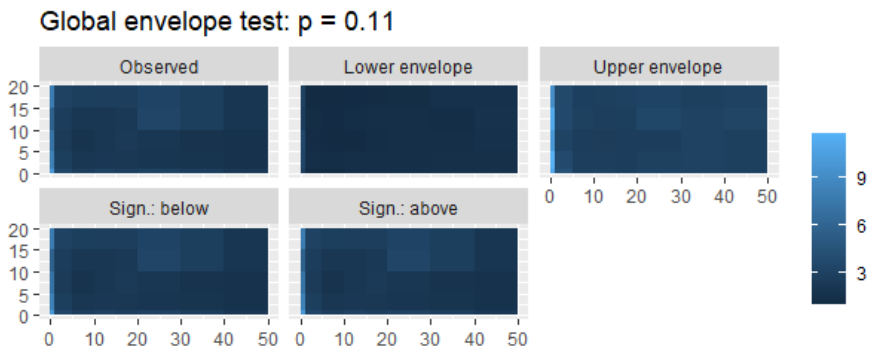

Figure 9: Graphical functional ERL envelope: the observed difference, the lower and upper bounds of the 95% global rank (ERL) envelope, and the significant regions (in red if any) where the observed coefficient goes below or above the envelope.

Conclusion

In this paper, we introduced the spatio-temporal Strauss hardcore point process. Strauss hardcore model is a Gibbs model for which points are pushed to be at a hardcore distance apart and repel up to a interaction distance which is larger than the hardcore distance. As in Raeisi et al. (2021), inference and simulation of the model were performed with logistic likelihood and birth-death Metropolis-Hasting algorithm, respectively. A multi-scale version of the model was introduced and applied to forest fires pattern to take into account structural complexity of forest fires in space and time. The model fitted very well the forest fire occurrences due to a model validation procedure using global envelopes and p-value of the spatio-temporal inhomogeneous pair correlation function based on the Extreme Rank Length (ERL) measure.

Because this model is suitable in an environmental and ecological framework, due to the complexity of mechanisms governing attraction and repulsion of entities (particles, cells, plants...), we can expect a wide use of it in many studies.

References

[1] Andersen, I. T., Hahn, U. (2016). Matérn thinned Cox processes. Spatial Statistics, **15**: 1–21.

[2] Baddeley, A., Coeurjolly, J. F., Rubak, E., Waagepetersen, R. (2014). Logistic regression for spatial Gibbs point processes. Biometrika, **101(2)**: 377–392.

[3] Baddeley, A., Rubak, E., Turner, R. (2015). Spatial Point Patterns: Methodology and Applications with `R`. Chapman and Hall/CRC Press, London.

[4] Baddeley, A., Turner, R. (2000). Practical maximum pseudolikelihood for spatial point patterns (with discussion). Australian and New Zealand Journal of Statistics, **42**: 283–322.

[5] Baddeley, A., Turner, R., Mateu, J., Bevan, A. (2013). Hybrids of Gibbs point process models and their implementation. Journal of Statistical Software, **55(11)**: 1–43.

[6] Baddeley, A., Rubak, E., Turner, R. (2019). Leverage and influence diagnostics for Gibbs spatial point processes. Spatial Statistics, **29**: 15–48.

[7] Badreldin, N., Uria-Diez, J., Mateu, J., Youssef, A., Stal, C., El-Bana, M., Magdy, A., Goossens, R. (2015). A spatial pattern analysis of the halophytic species distribution in an arid coastal environment. Environmental Monitoring and Assessment, **187**: 1-15.

[8] Cronie, O., van Lieshout, M. (2015). A J-function for inhomogeneous spatio-temporal point processes. Scandinavian Journal Statistics. **42(2)**: 562–579.

[9] Das, I., Stein, A. (2016). Application of the Multitype Strauss Point Model for Characterizing the Spatial Distribution of Landslides. Mathematical Problems in Engineering. `http://dx.doi.org/10.1155/2016/1612901`.

[10] Dereudre, D. (2019). Introduction to the theory of Gibbs point processes."In Stochastic Geometry. Lecture Notes in Mathematics vol. 2237, Coupier, D (Ed.). Springer, pp. 181–229.

[11] Dereudre, D., Lavancier, F. (2017). Consistency of likelihood estimation for Gibbs point processes, Annals of Statistics, **45(2)**: 744–770.

[12] Juan, P., Mateu, J. and Díaz-Avalos, C. (2010). Characterizing spatial-temporal forest fire Patterns. In METMA V: International Workshop on Spatio-Temporal Modelling. Santiago de Compostela, Spain.

[13] Hurtut, T., Landes, P. E., Thollot, J., Gousseau, Y., Drouilhet, R., Coeurjolly, J. F. (2009). Appearance-guided synthesis of element arrangements by example, Proceedings SIGGRAPH Symposium on Non-Photorealistic Animation and Rendering (NPAR), 51–60.

[14] Isham, V.S. (1984). Multitype Markov point processes: some approximations. Proceedings of the Royal Society of London, Series A, **391**: 39–53.

[15] Gabriel, E., Opitz, T., Bonneu, F. (2017). Detecting and modeling multiscale space-time structures: the case of wildfire occurrences. Journal de la Société Française de Statistique, **158(3)**: 86-105.

[16] Glass, L., Tobler, W. R. (1971). Uniform distribution of objects in a homogeneous field: Cities on a plain. Nature, **233**: 67-68.

[17] Gomez-Rubio, V. (2020). Bayesian Inference with INLA. Chapman & Hall-CRC, Boca Raton.

[18] Gonzalez, J. A., Rodriguez-Cortes, F. J., Cronie, O., Mateu, J. (2016). Spatio-temporal point process statistics: A review. Spatial Statistics, **18**: 505–544.

[19] Illian, J., Penttinen, A., Stoyan, H., Stoyan, D. (2008). Statistical Analysis and Modelling of Spatial Point Patterns, John Wiley & Sons, Chichester.

[20] Iftimi, A., van Lieshout, M. C., Montes, F. (2018). A multi-scale area-interaction model for spatio-temporal point patterns. Spatial Statistics, **26**: 38-55.

[21] Matérn, B. (1960). Spatial variation. Stochastic models and their application to some problems in forest surveys and other sampling investigations. Medd. Statens Skogsforskningsinst, **49(5)**: 1–144.

[22] Matérn, B. (1986). Spatial Variation. In: Lecture Notes in Statistics, vol. 36. Springer, New York.

[23] Mattfeldt, T., Eckel, S., Fleischer, F., Schmidt, V. (2006). Statistical analysis of reduced pair correlation functions of capillaries in the prostate gland. Journal of Microscopy, **223(2)**: 107–119.

[24] Mattfeldt, T., Eckel, S., Fleischer, F., Schmidt, V. (2007). Statistical modelling of the geometry of planar sections of prostatic capillaries on the basis of stationary Strauss hard-core processes. Journal of Microscopy, **228**: 272–281.

[25] Mattfeldt, T., Eckel, S., Fleischer, F., Schmidt, V. (2009). Statistical analysis of labelling patterns of mammary carcinoma cell nuclei on histological sections. Journal of Microscopy, **235**: 106–118.

[26] Møller, J., Waagepetersen, R. P. (2004). Statistical Inference and Simulation for Spatial Point Processes. Chapman and Hall/CRC, Boca Raton.

[27] Myllymäki, M., Kuronen, M., Mrkvička, T. (2020). Testing global and local dependence of point patterns on covariates in parametric models. Spatial Statistics, **42**: 100436.

[28] Myllymäki, M., Mrkvička, T. (2020). `GET`: Global envelopes in `R`. submitted to Journal of Statistical Software. http://arxiv.org/abs/1911.06583

[29] Myllymäki, M., Mrkvička, T., Grabarnik, P., Seijo, H., Hahn, U. (2017). Global Envelope Tests for Spatial Processes. Journal of the Royal Statistical Society: Series B, **79**: 381–404. doi:10.1111/rssb.12172.

[30] Ogata, Y., Tanemura, M. (1981). Estimation of interaction potentials of spatial point patterns through the maximum likelihood procedure. Annals of the Institute of Statistical Mathematics, **33**: 315–338.

[31] Papangelou, F. (1974). The conditional intensity of general point processes and an application to line processes. Probability Theory and Related Fields, **28(3)**: 207–226.

[32] R Core Team (2016). `R`: A Language and Environment for Statistical Computing. `R` Foundation for Statistical Computing, Vienna, Austria, `https://www.R-project.org/`.

[33] Raeisi, M., Bonneu, F., Gabriel, E. (2019). On spatial and spatio-temporal multi-structure point process models. Annales de l'Institut de Statistique de l'Université de Paris, **63(2-3)**: 97-114.

[34] Raeisi, M., Bonneu, F., Gabriel, E. (2021). A spatio-temporal multi-scale model for Geyer saturation point process: application to forest fire occurrences. Spatial Statistics, **41**: 100492.

[35] Ripley, B. D. (1988). Statistical Inference for Spatial Processes. Cambridge University Press.

[36] Ripley, B.D., Kelly, F.P. (1977). Markov point processes. Journal of the London Mathematical Society. **15(1)**: 188–192. `https://doi.org/10.1112/jlms/s2-15.1.188`

[37] Siino, M., Adelfio, G., Mateu, J., Chiodi, M., D'Alessandro, A. (2017). Spatial pattern analysis using hybrid models: an application to the Hellenic seismicity. Stochastic Environmental Research and Risk Assessment, **31(7)**: 1633-1648.

[38] Siino, M., D'Alessandro, A., Adelfio, G., Scudero, S., Chiodi, M. (2018). Multiscale processes to describe the eastern sicily seismic sequences. Annals of Geophysics, **61(2)**.

[39] Stoyan, D. (1992). Statistical estimation of model parameters of planar Neyman-Scott cluster processes. Metrika, **39(1)**: 67-74. `https://doi.org/10.1007/BF02613983`

[40] Stoyan, D. (2016). Point process statistics: application to modern and contemporary art and design. Journal of Mathematics and the Arts, **10**: 20–34.

[41] Sweeney, S., Gómez-Antonio, M. (2016). Localization and industry clustering econometrics: An assessment of Gibbs models for spatial point processes. Journal of Regional Science, **56**: 257–287.

[42] Taylor, D. B., Dhillon, H. S., Novlan, T. D., Andrews, J. G. (2012). Pairwise interaction processes for modeling cellular network topology. Proceedings IEEE GLOBECOM in Anaheim.

[43] Teichmann, J., Ballani, F. and Boogaart, K.G. van den (2013). Generalizations of Matern's hard-core point processes. Spatial Statistics, **9**: 33–53.

[44] Turner, R. (2009). Point patterns of forest fire locations. Environmental and Ecological Statistics, **16**: 197–223. https://doi.org/10.1007/s10651-007-0085-1

[45] van Lieshout, M.N.M. (2002). Markov Point Processes and Their Applications. Imperial College Press, London.

[46] Wang, X., Zheng, G., Yun, Z., Moskal, L.M. (2020). Characterizing tree spatial distribution patterns using discrete Aerial Lidar Data. Remote Sensing , **12(4)**, 712. https://doi.org/10.3390/rs12040712

[47] Ying, Q., Zhao, Z., Zhou, Y., Li, R., Zhou, X., Zhang, H. (2014). Characterizing spatial patterns of base stations in cellular networks. Proceedings IEEE/CIC International Conference on communications in China (ICCC), 490-495.